Dictyostelium Myosin II Mutations That Uncouple the Converter Swing and ATP Hydrolysis Cycle†

Naoya Sasaki,‡ Reiko Ohkura,§ and Kazuo Sutoh*,§

Center for Interdisciplinary Research, Tohoku University, Aramaki-aza-aoba, Aoba-ku, Sendai, Miyagi 980-8579, Japan, and Department of Life Sciences, Graduate School of Arts and Sciences, University of Tokyo, Komaba 3-8-1, Meguro-ku, Tokyo 153-8902, Japan

Received April 30, 2002; Revised Manuscript Received October 22, 2002

ABSTRACT: During the ATP hydrolysis cycle of the *Dictyostelium* myosin II motor domain, two conserved α-helices, the SH1/SH2 helix and the relay helix, rotate in a coordinated way to induce the swing motion of the converter domain. A network of hydrophobic and ionic interactions in these two helices and the converter may ensure that the motions of these helices are effectively transmitted to the converter. To examine the roles of these interactions in the ATPase-dependent converter swing, we disrupted two conserved hydrophobic linkages among them by means of a point mutation (I499A or F692A). The resulting mutations induced only limited changes in the kinetic parameters of ATP hydrolysis, except for a marked increase of basal MgATPase activity. However, the mutant myosins completely lost their in vitro and in vivo motor functions. Measurements of the intrinsic tryptophan fluorescence and the GFP-based FRET revealed that the converter domain of these mutants did not swing during steady-state ATP hydrolysis or in the presence of tightly trapped Mg·ADP·V_i, which shows that the point mutations induced the uncoupling of the converter swing and ATP hydrolysis cycle. These results highlight the importance of these hydrophobic linkages for transmitting the coordinated twist motions of the helices to the converter as well as the requirement of this converter swing for force generation.

The ATP hydrolysis cycle of *Dictyostelium* myosin II proceeds as follows (*1*−*3*). Myosin first forms an unstable collision complex with ATP (the M·ATP state), and then binds it tightly to take the M^+·ATP state, which is characterized by its quenched tryptophan fluorescence. Myosin then undergoes the isomerization step to take the M*·ATP state, which is characterized by its enhanced tryptophan fluorescence. Quick hydrolysis of ATP generates the most stable intermediate state, i.e., the M*·ADP·P_i[1] state, which is equivalent to the M**·ADP·P_i state of vertebrate skeletal muscle myosin (*4*). The phosphate generated by this ATP hydrolysis is then slowly released from the back door of the ATPase pocket (*5*). The myosin then takes the M^+·ADP state. After the release of ADP, myosin becomes ready for another cycle of ATP hydrolysis. Since the transition from the prestroke structure to the poststroke structure occurs at the P_i-release step and the backward transition occurs at the isomerization step (*6*), we designate the intermediate states after the isomerization step and before the P_i-release step as the "prestroke state" and the remaining ones as the "poststroke state." As far as the ATPase site is concerned, its "back door" is closed to be ready for ATP hydrolysis in the prestroke state, while it is open in the poststroke state (*1*−*3*, *7*).

Two types of crystal structures of the motor domain of *Dictyostelium* myosin (designated as S1dC) may represent intermediate structures of this ATP hydrolysis cycle (*7*, *8*). One is the putative "poststroke structure" derived from S1dC with bound Mg·ADP or Mg·ADP·BeF_x. The other is the putative "prestroke structure" derived from S1dC with bound Mg·ADP·AlF_4 or Mg·ADP·V_i. These crystal structures have revealed that, upon the transition from the poststroke to the prestroke structure, the switch II loop locating at the bottom of the ATPase pocket changes its conformation around the "phosphate sensor" G457 (*9*). These conformational changes are finally transmitted to the converter domain, which is expected to rotate by ∼70° on the prestroke/poststroke transition (*6*, *10*). It is generally assumed that this rotation of the converter is amplified as a long-distance swing of the lever arm along an actin filament (*10*).

The converter domain is held in its position by the two conserved α-helices, the SH1/SH2 helix, and the relay helix (Figure 1). The network of many ionic and hydrophobic interactions in these helices and the converter ensures the coordinated twisting motions of these helices and efficient transmission of these motions to the converter. The SH1/SH2 helix is covalently connected to the converter domain through the highly conserved G691-F692 motif (hereafter, residue numbers are for *Dictyostelium* myosin II). The main chain of the SH1/SH2 helix rotates at the conserved G680 as well as at the G691-F692 motif on the prestroke/poststroke

† This work was supported by grants-in-aid for Scientific Research from the Ministry of Education, Science, Sports, and Culture of Japan to K.S. and from the Japan Society for the Promotion of Science for Young Scientists to N.S.

* To whom correspondence should be addressed: telephone/fax, 81-3-5454-6751; e-mail, sutoh@bio.c.u-tokyo.ac.jp.

‡ Tohoku University.

§ University of Tokyo.

[1] Abbreviations: S1, subfragment 1 of *Dictyostelium* myosin II; S1dC, S1 without the C-terminal lever-arm domain; Mant, 2′(3′)-*O*-(*N*-methylanthraniloyl); P_i, inorganic phosphate; V_i, inorganic vanadate.

10.1021/bi026051l CCC: $25.00
Published on Web 12/14/2002

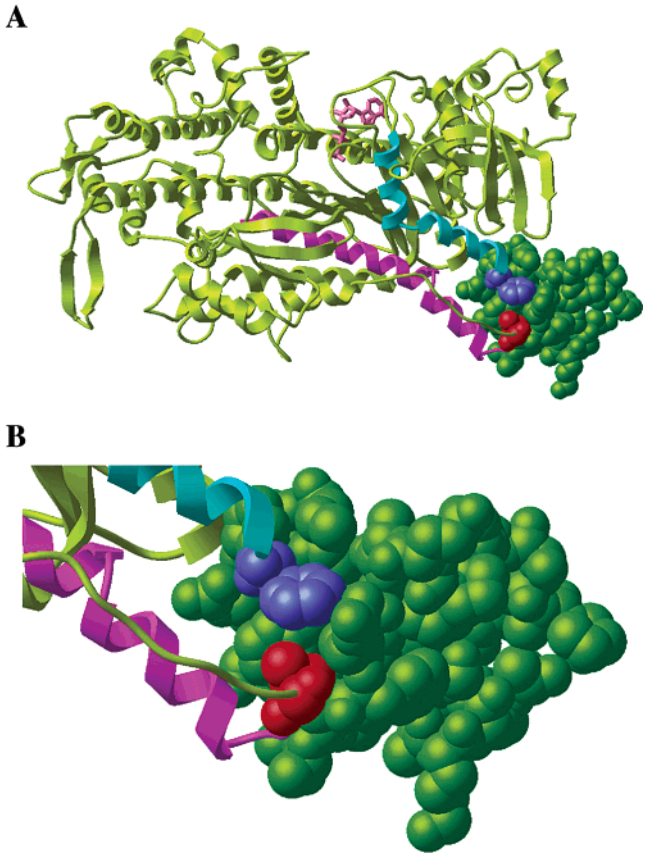

FIGURE 1: (A) Crystal structures of the myosin motor domain complexed with Mg·ADP·V_i. I499 and F692 are shown as space-filling models and colored in red and blue, respectively. The relay helix is shown as a magenta ribbon and the SH1/SH2 helix as a cyan ribbon. The converter is shown in green. (B) A closeup view around I499 and F692.

transition (*7*, *8*). The side chain of F692 that maintains a hydrophobic contact with the core of the converter may work as an anchor, transmitting the twisting motion of the SH1/SH2 helix to the converter.

The relay helix is a long α-helix that connects the switch II loop and the side of the converter domain. On the prestroke/poststroke transition, small ATPase-dependent conformational changes induced at the switch II loop are propagated to the relay helix as its twisting motion. The C-terminal end of the relay helix is in contact with the side of the converter through a network of interactions, among which a hydrophobic linkage between I499 in the helix and a residue (E738 for *Dictyostelium* myosin II) in the converter domain is very much conserved and is maintained during the converter swing (*11*).

To verify the importance of these hydrophobic linkages at I499 and F692 in the converter swing and force generation, we disrupted them by introducing a point mutation (I499A and F692A) in *Dictyostelium* myosin II and carried out detailed in vivo and in vitro analyses of these mutants.

EXPERIMENTAL PROCEDURES

Construction and Expression of Mutant Myosins and Their Fragments. Mutagenesis and construction of plasmids of mutant full-length myosins and their fragments were carried out as described (*12*, *13*). Briefly, I499 or F692 was changed to alanine by site-directed mutagenesis (*14*) of the *Dictyostelium* myosin II heavy chain gene (*15*). Mutant myosin genes were sequenced and then ligated with the *Dictyostelium* actin-15 promoter by using a *Bam*HI site generated as the junction of the promoter and the heavy chain gene. As a result, the N-terminal sequence of the heavy chain was changed to M-D-P- from the original sequence M-N-P-. A *Sac*I site was also introduced after the stop codon as the junction of the heavy chain gene and the actin-6 terminator. The resulting construct was finally ligated between the *Xba*I and *Sac*I sites in the pBIG vector (*16*, *17*), in which the actin-6 terminator with a unique *Sac*I site at its 5′ end had been inserted. By means of electroporation, these plasmids were introduced into *Dictyostelium* cells in which the heavy chain gene had been knocked out by homologous recombination (myosin-null cells) (*18*). The transformants were selected in an HL-5 medium (*19*) supplemented with penicillin/streptomycin and 20 μg/mL G418 on plastic dishes for 1 week.

The truncated myosin heavy chain genes corresponding to myosin subfragment 1 (S1) were constructed as follows. The heavy chain was truncated at E836 by introducing a stop codon at the corresponding location of the heavy chain gene. A unique *Sac*I site was introduced after the stop codon as the junction between the S1 gene and the terminator. After the actin-15 promoter and actin-6 terminator werre fused, two *Not*I sites were further added at the 5′ and 3′ ends. The S1 construct was inserted into a unique *Not*I site of the pTIKLOE vector (*20*) that carries the essential and regulatory light chain genes (*21*) driven by the actin-15 promoter. The 5′ end of the regulatory light chain gene was modified so that the expressed light chain carried the histidine tag (His_6) at its N-terminus. Transformations were carried out by using *Dictyostelium* AX2 cells. Transformants were selected as above.

The GFP/BFP fusion of S1dC of *Dictyostelium* myosin II was constructed as described (*6*). The myosin heavy chain gene was truncated at Q758 (*22*) and then ligated with the enhanced BFP gene through a linker that corresponds to the Gly-Gly-Gly sequence. The red-shifted GFP gene was ligated at the 5′ *Bam*HI site of the truncated myosin gene through a linker corresponding to the Gly-Pro-Gly sequence. Between the actin promoter and the GFP gene, the His-tag sequence was introduced as a double-stranded oligonucleotide so that the expressed GFP/BFP fusion protein had the N-terminal His tag. The resulting fusion gene was finally inserted into the pBIG vector modified as above. Transformation of AX2 cells and selection of transformants were carried out as above.

Phenotypes of Transformed Cells. The growth rates of cells expressing the recombinant myosins were measured in suspension as described (*12*). The spore formation of transformed cells was examined on agar plates as described (*12*).

Protein Purification. Full-length myosin was purified as described (*12*). The phosphorylation of purified myosin was carried out by using the recombinant *Dictyostelium* myosin light chain kinase (MLCK) as described (*16*, *23*).

Mutant S1s and GFP/BFP fusion proteins were prepared as described (*6*, *24*) with some modifications. Truncated protein was extracted from transformed *Dictyostelium* cells and precipitated as the complex with F-actin, as described for the full-length myosin (*12*). It was then extracted from the precipitate with a solvent comprising 10 mM MOPS,

pH 7.4, 250 mM NaCl, 7 mM $MgCl_2$, and 5 mM ATP. The extract was directly applied to an NTA-Ni agarose column (Qiagen). After the column was washed with one column volume of the above solvent supplemented with 1 mM ATP, the protein was eluted with 200 mM imidazole, pH 7.4. The eluted fractions were collected, dialyzed against a solvent comprising 50 mM NaCl, 10 mM MOPS, pH 7.4, and 2 mM $MgCl_2$, and then centrifuged at 100000 rpm × 30 min (Beckman TL100-3) before use.

F-actin was extracted from the acetone powder of rabbit skeletal muscle and purified as described (*25*).

ATPase Assays. Actin-activated and basal MgATPase activities were measured as described (*26*) with some modifications. Purified full-length myosin (20−50 μg/mL) and various concentrations of F-actin (0−0.5 mg/mL) were mixed in an assay buffer comprising 18 mM MOPS, pH 7.4, 12.5 mM KCl, 35 mM NaCl, and 5 mM $MgCl_2$. The reactions were started by adding $^1/_{10}$ volume of 10 mM ATP and stopped by adding 4 volumes of 0.3 M PCA. The assays were carried out at 25 °C.

Fast Kinetics. Binding or release of a mant nucleotide to and from wild-type or mutant S1 was followed by a stopped-flow apparatus with a fluorescence detector (Applied Photophysics, SX18) (*24*, *27*). Rate constants were calculated by using previously described equations (*28*−*31*).

Spectra of Intrinsic Tryptophan Fluorescence. The fluorescence spectra of intrinsic tryptophan of the wild-type and mutant S1s were obtained in a solvent comprising 50 mM NaCl, 10 mM MOPS (pH 7.4), and 2 mM $MgCl_2$ in the presence or absence of a nucleotide by a fluorometer (Perkin-Elmer LS50B) at $\lambda_{ex} = 290$ nm.

Trapping of a Nucleotide in the ATPase Site. Wild-type or mutant S1 (1 μM) in 50 mM NaCl, 10 mM MOPS (pH 7.4), and 2 mM $MgCl_2$ was mixed with 100 μM sodium vanadate and incubated at 25 °C for 30 min. Then, mant-ADP was added into each mixture to reach a final concentration of 10 μM. After the mixture was incubated at 25 °C for 30 min, ATP was added to each sample to reach a final concentration of 1 mM in order to chase the bound mant-ADP in the ATPase site. After addition of ATP, the fluorescence intensity of mant-ADP ($\lambda_{ex} = 295$ nm, $\lambda_{em} = 440$ nm) was followed by a fluorometer (Perkin-Elmer LS50B). When chased from the ATPase site of myosin, the fluorescence intensity of mant-ADP decreased.

GFP−FRET Measurements. GFP-based FRET (fluorescence resonance energy transfer) measurements were carried out in 50 mM NaCl, 10 mM MOPS (pH 7.4), and 2 mM $MgCl_2$ by exciting BFP at 360 nm or GFP at 480 nm as previously described (*6*). FRET efficiencies (*E*) were determined from the sensitized emission of GFP according to the equation (*32*):

$$E = \{(\text{ratio})^A - \epsilon^A(360)/\epsilon^A(480)\}\{\epsilon^A(480)/\epsilon^D(360)\}$$

where superscripts D and A refer to donor (BFP) and acceptor (GFP) and $\epsilon^A(360)$, $\epsilon^A(480)$, and $\epsilon^D(360)$ to molar extinction coefficients of donor and acceptor at the designated wavelength. $(\text{ratio})^A$ is the emission ratio of acceptor defined as $(\text{ratio})^A = F^A_{FRET}/F^A_{DIR}$, where F^A_{FRET} is the fluorescence intensity of the acceptor (GFP) at 510 nm when the donor (BFP) is excited and F^A_{DIR} is the fluorescence intensity of the acceptor (GFP) at 510 nm when it is directly excited at 480 nm.

In Vitro Motility Assays. In vitro motility assays were carried out as previously described (*33*, *34*) with some modifications. Purified full-length myosin was introduced into a chamber constructed from silicone-coated cover glasses. The assay buffer comprised 25 mM imidazole, pH 7.4, 4 mM $MgCl_2$, 1 mM DTT, 0.2% methylcellulose, and O_2 scavengers (*35*). F-actin was labeled with rhodamine/phalloidin. The assays were carried out at 25 °C.

Table 1: In Vitro Motor Activities of Wild-Type and Mutant Myosins

	in vitro motility[a] (μm/s)	basal Mg-ATPase (s^{-1})	actin-activated Mg-ATPase (s^{-1})
WT	1.45 ± 0.26	0.05 ± 0.01	2.06 ± 0.11
I499A	not motile	0.36 ± 0.05	1.28 ± 0.01
F692A	not motile	0.35 ± 0.04	0.63 ± 0.05

[a] Sliding velocities of actin filaments were determined in the presence of 0.2% methylcellulose.

Table 2: Kinetic Parameters of Wild-Type and Mutant S1s

	WT	I499A	F692A
mant-ATP binding ($\mu M^{-1}\cdot s^{-1}$)	1.54	1.08	0.58
mant-ADP release (s^{-1})	1.03	4.66	1.42
mant-ADP binding ($\mu M^{-1}\cdot s^{-1}$)	0.83	0.67	0.33

RESULTS

Mutant Myosins Have Defects in Motor Functions. The expression of a full-length myosin II gene in *Dictyostelium* myosin-null cells is a simple and direct assay for its in vivo motor functions (*36*). The myosin-null cells expressing either I499A or F692A myosin exhibited phenotypes similar to those of the parental myosin-null cells: they neither formed spores when starved nor grew in a suspension culture (data not shown). The results indicate that both of these mutant myosins lost their in vivo motor functions.

Consistent with these in vivo defects, the in vitro motility assays of purified I499A or F692A myosin showed that they completely lost the ability to drive the sliding motion of actin filaments (Table 1).

ATPase Kinetics of Purified Myosins and Their S1 Fragments. Although complete loss of in vivo and in vitro motility was observed for I499A and F692A myosins, these full-length myosins still exhibited basal MgATPase activity that was higher than that of the wild type (0.36 ± 0.05 s^{-1} for I499A, 0.35 ± 0.04 s^{-1} for F692A, and 0.05 ± 0.01 s^{-1} for the wild type) (Table 1). Moreover, these mutants retained actin-activated ATPase activity, though lower than that of the wild type (1.28 ± 0.01 s^{-1} for I499A, 0.63 ± 0.05 s^{-1} for F692A, and 2.06 ± 0.11 s^{-1} for the wild type) (Table 1). Their K_m values of actin-activated MgATPase activity were not significantly different from the K_m value of the wild type.

The second-order rate constants for mant-ATP or mant-ADP binding to the mutant S1s were measured. These values were similar to those of wild-type S1, although some deviations were observed (Table 2). The rates of mant-ADP release from the mutant S1s also showed some deviations from the rate of the wild type. However, it must be noted that the ADP-release rate was faster than the P_i-release rate

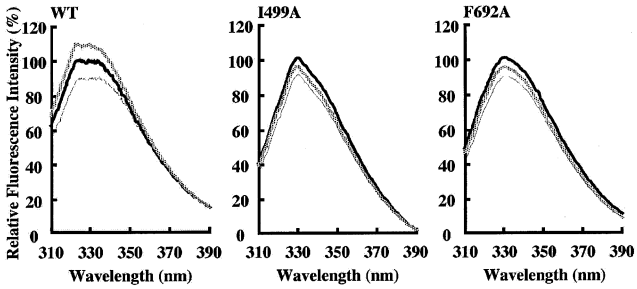

FIGURE 2: Tryptophan fluorescence of wild-type and mutant S1s. Fluorescence spectra were obtained in the absence of nucleotide (solid line), in the presence of 1 mM ATP (dashed line), and in the presence of 1 mM ADP (dotted line). Solvent conditions: 10 mM MOPS (pH 7.4), 50 mM NaCl, and 2 mM $MgCl_2$. Excitation: 290 nm.

Table 3: FRET Efficiency of Wild-Type and Mutant GFP/BFP Fusion Proteins

	no nucleotide	ATP	ADP	ADP·V_i
WT	0.50 ± 0.06	0.16 ± 0.01	0.38 ± 0.01	0.12 ± 0.01
I499A	0.55 ± 0.03	0.49 ± 0.02	0.60 ± 0.01	0.48 ± 0.01
F692A	0.55 ± 0.01	0.48 ± 0.01	0.56 ± 0.01	0.43 ± 0.01

(the basal ATPase activity) for both of the mutants, especially for I499A, indicating that the P_i-release step is the rate-limiting step of the steady-state ATPase reaction for the wild type as well as for these mutants.

Defect of the Converter Swing during Steady-State ATP Hydrolysis. As shown in Figure 2, intrinsic tryptophan fluorescence increased upon addition of excess ATP to the wild-type S1. It is generally assumed that this increase of fluorescence intensity mainly reflects the converter swing to the prestroke orientation from the poststroke orientation. Upon addition of excess ATP to I499A or F692A S1, however, the intrinsic tryptophan fluorescence did not increase but, rather, decreased. A similar level of decrease of the tryptophan fluorescence was detected upon addition of ADP to these mutants, as in the case of the wild type. These results imply that the converter domain of these mutants remained in the poststroke orientation during steady-state ATP hydrolysis.

To further confirm this notion, we directly examined whether the converter domain of I499A or F692A myosin swings during ATP hydrolysis by using the GFP-based FRET measurement on the fusion proteins of GFP, BFP, and S1dC as previously described (*6*). In the absence of a nucleotide, the FRET efficiency between GFP and BFP attached to the N- and C-termini of I499A or F692A S1dC was 0.55 (Table 3). Since the FRET efficiency for the wild-type fusion protein in the absence of a nucleotide, i.e., at the poststroke state, was 0.50 as compared to 0.16 in the presence of excess ATP, i.e., at the prestroke state, it is likely that the converter of these mutants took a poststroke orientation similar to that of the wild type. Unlike the wild type, however, the FRET efficiency of the I499A or F692A mutant remained at the level of the poststroke structure (0.48−0.49) even in the presence of excess ATP (Table 3), supporting the above notion that the converter remained in the poststroke orientation during steady-state ATP hydrolysis.

Defect of the Converter Swing at the State Trapped with Mg·ADP·V_i. The result above in which the converter remained in the poststroke orientation during steady-state

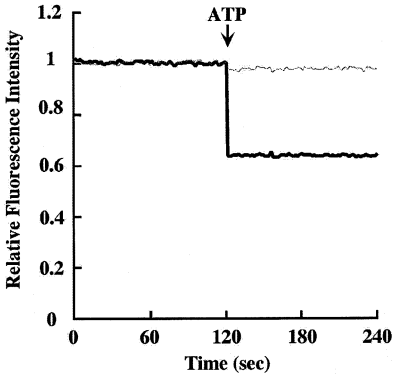

FIGURE 3: ATP chase of mant-ADP bound to the wild-type (WT) S1. The WT S1 was mixed with mant-ADP in the presence or absence of V_i, and the bound nucleotide was then chased upon addition of excess ATP. In the absence of V_i (solid line), the fluorescence intensity of the mant moiety quickly dropped due to its dissociation from the ATPase site. In the presence of V_i (dashed line), the fluorescence intensity did not change upon addition of ATP since ATP did not chase the tightly bound mant-ADP.

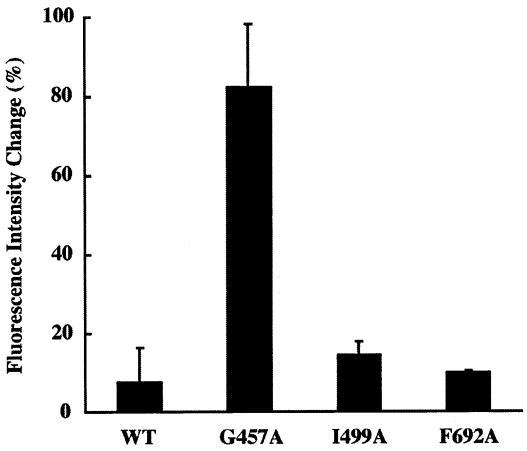

FIGURE 4: Trapping of mant-ADP by the wild-type and mutant S1s. ATP-chase experiments, as in Figure 3, were carried out for the wild-type (WT), G457A, I499A, and F692A S1s in the presence of V_i. As controls, similar experiments were carried out in the absence of V_i. The amount of mant-ADP chased by ATP for each experiment is shown as a bar representing the fluorescence intensity change upon addition of ATP (%) that is normalized by the value observed in the absence of V_i. A smaller value means a tighter trap of the bound mant-ADP.

ATP hydrolysis could be due to a kinetic effect, i.e., the accumulation of mutant molecules in the M^+·ATP state, i.e., in the poststroke state. We examined this possibility by trapping the ATPase cycle of the mutants at the prestroke state with Mg·ADP·V_i.

First, the binding of mant-ADP to S1 was examined by exploiting the fact that the fluorescence intensity of the mant moiety is enhanced when mant-ADP binds in the ATPase site (*37*−*39*). When excess ATP was added to the wild-type S1 that had bound to mant-ADP, the weakly bound nucleotide was easily chased, resulting in a quick decrease of the fluorescence (Figure 3). However, in the presence of V_i, the fluorescence only slightly decreased upon addition of excess ATP because the mant-ADP was tightly trapped in the ATPase site as the complex with V_i and was hardly chased by ATP. When G457A S1 was used in place of the wild type, mant-ADP was not tightly trapped even in the presence of V_i, as shown in Figure 4. This result is consistent with the fact that the G457A mutant cannot take the prestroke

state in the presence of ATP since its ATPase cycle is blocked before the isomerization step (*13*). Unlike the G457A mutant, similar trap experiments on I499A and F692A S1s showed that both of them tightly bound to mant-ADP in the presence of V_i (Figure 4). The results indicate that, under the conditions, the ATPase site of the I499A or F692A mutant was fixed at the prestroke state with tightly bound Mg·ADP·V_i.

By means of the GFP-based FRET measurement, we then examined whether the converter of the I499A or F692A mutant ever adopted the prestroke orientation when the ATPase site was fixed at the prestroke state. As shown in Table 3, the FRET efficiency between GFP and BFP of the I499A or F692A mutant with the tightly bound Mg·ADP·V_i was very similar to that observed in the absence of a nucleotide. Thus, even when the ATPase site of these mutants was fixed at the prestroke state, their converter did not take the prestroke orientation but, rather, took the poststroke orientation. Under the same conditions, the converter of the wild type took the prestroke orientation, as previously described (*6*).

DISCUSSION

Like the wild-type myosin, the I499A or F692A myosin normally associated to and dissociated from the actin filament, depending on the steps of the ATP hydrolysis cycle. The actin activation of myosin ATPase activity was also maintained to some extent for both of the mutants, especially for I499A. Moreover, the steady-state and transient kinetic analyses of ATP hydrolysis by I499A and F692A mutants showed no dramatic change in the hydrolysis steps, except for the increase of basal MgATPase activity. However, these mutants lost their in vivo and in vitro motor functions. Consistently with these defects, the intrinsic tryptophan fluorescence of these mutants did not show any enhancement during the steady-state ATP hydrolysis. Furthermore, the GFP-based FRET measurements of the GFP/BFP fusion of I499A or F692A S1dC also showed that the converter remained in the poststroke orientation even in the presence of excess ATP.

One possibility for these observations is that the mutant molecules are accumulated before the isomerization step and, therefore, the converter takes the poststroke orientation most of the time even in the presence of excess ATP. Another possibility is that the converter takes the poststroke orientation even when the mutants are in the prestroke state, i.e., in intermediate states between the isomerization and P_i-release steps. Judging from the observation that the converters of these mutants took the poststroke orientation even when the mutants were fixed in the prestroke state with the tightly bound Mg·ADP·V_i, the latter is more likely. This implies that, during the steady-state ATP hydrolysis, the converter of I499A or F692A remained in the poststroke orientation even when the ATPase site took the prestroke state with its back door closed in preparation for ATP hydrolysis. Once the critical hydrophobic linkage between the relay helix and the converter was disrupted by I499A mutation, the twisting motion of the relay helix would no longer be transmitted to the converter. The F692A mutation also disrupted another critical hydrophobic linkage maintaining the contact between the SH1/SH2 helix and the converter. This mutation would thereby uncouple the twisting motion of the SH1/SH2 helix and the converter swing. Thus, either the I499A mutation or the F692A mutation resulted in a complete uncoupling of the converter swing and the ATP hydrolysis cycle; the ATPase cycle of these mutants proceeded rather normally without the converter swing. This defect in the converter swing during the ATP hydrolysis cycle may be the direct cause of the loss of the in vivo and in vitro motor functions of these mutants.

These results highlight the importance of these critical hydrophobic contacts at I499 and F692 for transmitting the coordinated twist motions of the helices to the converter as well as the requirement of this converter swing for force generation.

ACKNOWLEDGMENT

The myosin II heavy chain gene, the myosin-null cell, the pBIG and the pTIKLOE vectors, and the recombinant MLCK gene were kindly supplied by Dr. J. A. Spudich (Stanford University), Dr. B. Patterson (University of Arizona), and Dr. T. Q. P. Uyeda [Gene Discovery Research Center, National Institute of Advanced Industrial Science and Technology (AIST), Japan]. We thank Dr. T. Hiratsuka (Asahikawa Medical College, Japan) for providing us with mant-ADP and mant-ATP.

REFERENCES

1. Malnasi-Csizmadia, A., Woolley, R. J., and Bagshaw, C. R. (2000) *Biochemistry 39*, 16135−16146.
2. Malnasi-Csizmadia, A., Pearson, D. S., Kovacs, M., Woolley, R. J., Geeves, M. A., and Bagshaw, C. R. (2001) *Biochemistry 40*, 12727−12737.
3. Malnasi-Csizmadia, A., Kovacs, M., Woolley, R. J., Botchway, S. W., and Bagshaw, C. R. (2001) *J. Biol. Chem. 276*, 19483−19490.
4. Bagshaw, C. R., and Trentham, D. R. (1974) *Biochem. J. 141*, 331−349.
5. Yount, R. G., Lawson, D., and Rayment, I. (1995) *Biophys. J.* 44S−47S (discussion 47S−49S).
6. Suzuki, Y., Yasunaga, T., Ohkura, R., Wakabayashi, T., and Sutoh, K. (1998) *Nature 396*, 380−383.
7. Smith, C. A., and Rayment, I. (1996) *Biochemistry 35*, 5404−5417.
8. Fisher, A. J., Smith, C. A., Thoden, J. B., Smith, R., Sutoh, K., Holden, H. M., and Rayment, I. (1995) *Biochemistry 34*, 8960−8972.
9. Smith, C. A., and Rayment, I. (1996) *Biophys. J. 70*, 1590−1602.
10. Holmes, K. C. (1997) *Curr. Biol. 7*, 112−118.
11. Shih, W. M., and Spudich, J. A. (2001) *J. Biol. Chem. 276*, 19491−19494.
12. Shimada, T., Sasaki, N., Ohkura, R., and Sutoh, K. (1997) *Biochemistry 36*, 14037−14043.
13. Sasaki, N., Shimada, T., Ohkura, R., and Sutoh, K. (1998) *J. Biol. Chem. 273*, 20334−20340.
14. Kunkel, T. A. (1985) *Proc. Natl. Acad. Sci. U.S.A. 82*, 488−492.
15. DeLozanne, A., Lewis, M., Spudich, J. A., and Leinwand, L. A. (1985) *Proc. Natl. Acad. Sci. U.S.A. 82*, 6807−6810.
16. Ruppel, K. M., Uyeda, T. Q., and Spudich, J. A. (1994) *J. Biol. Chem. 269*, 18773−18780.
17. Patterson, B., and Spudich, J. A. (1995) *Genetics 140*, 505−515.
18. Manstein, D. J., Titus, M. A., De, L. A., and Spudich, J. A. (1989) *EMBO J. 8*, 923−932.
19. Sussman, M. (1987) *Methods Cell Biol. 28*, 9−29.
20. Uyeda, T. Q., Tokuraku, K., Kaseda, K., Webb, M. R., and Patterson, B. (2002) *Biochemistry 41*, 9525−9534.
21. Chisholm, R. L., Rushforth, A. M., Pollenz, R. S., Kuczmarski, E. R., and Tafuri, S. R. (1988) *Mol. Cell. Biol. 8*, 794−801.
22. Itakura, S., Yamakawa, H., Toyoshima, Y. Y., Ishijima, A., Kojima, T., Harada, Y., Yanagida, T., Wakabayashi, T., and Sutoh, K. (1993) *Biochem. Biophys. Res. Commun. 196*, 1504−1510.

23. Tan, J. L., and Spudich, J. A. (1991) *J. Biol. Chem. 266*, 16044−16049.
24. Sasaki, N., Asukagawa, H., Yasuda, R., Hiratsuka, T., and Sutoh, K. (1999) *J. Biol. Chem. 274*, 37840−37844.
25. Spudich, J. A., and Watt, S. (1971) *J. Biol. Chem. 246*, 4866−4871.
26. Kodama, T., Fukui, K., and Kometani, K. (1986) *J. Biochem. (Tokyo) 99*, 1465−1472.
27. Sasaki, N., Ohkura, R., and Sutoh, K. (2000) *J. Biol. Chem. 275*, 38705−38709.
28. Ritchie, M. D., Geeves, M. A., Woodward, S. K., and Manstein, D. J. (1993) *Proc. Natl. Acad. Sci. U.S.A. 90*, 8619−8623.
29. Woodward, S. K., Geeves, M. A., and Manstein, D. J. (1995) *Biochemistry 34*, 16056−16064.
30. Kurzawa, S. E., Manstein, D. J., and Geeves, M. A. (1997) *Biochemistry 36*, 317−323.
31. Kuhlman, P. A., and Bagshaw, C. R. (1998) *J. Muscle Res. Cell Motil. 19*, 491−504.
32. Clegg, R. M. (1992) *Methods Enzymol. 211*, 353−388.
33. Kron, S. J., and Spudich, J. A. (1986) *Proc. Natl. Acad. Sci. U.S.A. 83*, 6272−6276.
34. Toyoshima, Y. Y., Kron, S. J., McNally, E. M., Niebling, K. R., Toyoshima, C., and Spudich, J. A. (1987) *Nature 328*, 536−539.
35. Harada, Y., Sakurada, K., Aoki, T., Thomas, D. D., and Yanagida, T. (1990) *J. Mol. Biol. 216*, 49−68.
36. Egelhoff, T. T., Manstein, D. J., and Spudich, J. A. (1990) *Dev. Biol. 137*, 359−367.
37. Woodward, S. K., Eccleston, J. F., and Geeves, M. A. (1991) *Biochemistry 30*, 422−430.
38. Hiratsuka, T. (1983) *Biochim. Biophys. Acta 742*, 496−508.
39. Bauer, C. B., Kuhlman, P. A., Bagshaw, C. R., and Rayment, I. (1997) *J. Mol. Biol. 274*, 394−407.

BI026051L